Precise Time and Frequence Transfer

D. Matsakis[1], P. Defraigne[2], and P. Banerjee[3]

[1]US Naval Observatory (USNO)
Washington, DC, USA
E-mail: demetrios.matsakis@usno.navy.mil

[2]Royal Observatory of Belgium
Brussels, Belgium
E-mail: p.defraigne@oma.be

[3]ECE, ASET
Amity University, Noida, India
E-mail: pbanerjee150@gmail.com

Abstract

This article reviews modern time- and frequency-transfer technologies. The several techniques differ in precision, accuracy, complexity, and cost, and can be considered complementary. The paper discusses the current status and future developments of these techniques.

1. Introduction

In the last few decades, as atomic frequency standards have attained greater precision and accuracy, the precision and accuracy of operational time-transfer modes have improved in parallel. This development was driven by the fact that even a perfect clock would be of little use if its time could not be distributed to users, who have a variety of robustness, accuracy, and precision requirements (RAPRS). In order to assure reliable time to their users, the timing laboratories themselves must meet a more-stringent standard than any of their end-user's requirements. The most demanding requirements come from space systems, notably global navigation satellite systems (GNSS), the end-to-end robustness, accuracy, and precision requirements of which for internal operations and interoperability are currently at the level of one nanosecond. Ground-based navigational systems that serve as backups or supplements would in principle have the same requirements; however, the presence of other sources of error can mask their time-transfer noise. In general, the robustness, accuracy, and precision requirements of satellite communication systems are at the microsecond level, and this is consistent with the ITU frequency specification of 1.E-11. The financial communities have a need for accurate time-stamping and pc synchronization. In the United States, the official specification is effectively one second [1], although some financial brokers have asked for considerably more-accurate synchronization. So as to be able to reliably meet the demands of their users, the timing labs themselves have robustness, accuracy, and precision requirements that would best exceed those of their most critical users by an order of magnitude.

This review concentrates on the status and future of three fully operational systems at this time: network time protocol (NTP); two-way satellite time and frequency transfer (TWSTFT, also known as TWSTT); and GPS (which can be considered as a model for other GNSS systems, such as GLONASS, GALILEO, and BEIDOU). We very briefly discuss fiber-optic technology, which although only operational on links used for the generation of International Atomic Time (TAI) [2], promises the greatest precision of all; and long-range radio navigation (LORAN), which is finding a new value as a backup to GNSS. Although this review attempts to describe the performance of the several techniques at their current level of operational maturity, they are all improving, as will be necessary for future applications such as the evaluation of atomic fountains. Atomic fountains can now achieve operational precisions at the level of 1.E-16 over days if not months [3], and in the next decade, optical frequency standards are expected to be up to two orders of magnitude quieter [4, 5].

2. Network Time Protocol, or NTP

Network time protocol is an Internet-based hierarchal time-transfer technique in which client computers exchange time-labeled packets with servers. Servers receiving their time independently of network time protocol, such as
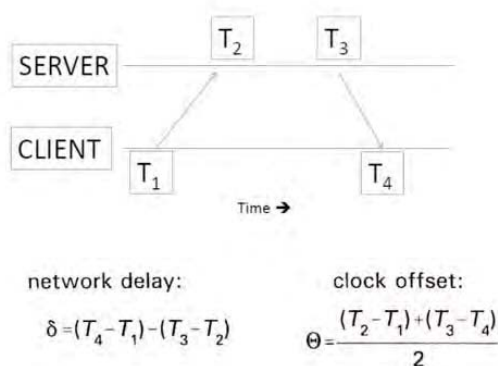
Figure 1. A schematic diagram of network time protocol time transfer. The Ts represent the times of transmission/reception as measured by the local clock, and the formulas show how the time difference and network delay are computed.

network delay:

$$\delta = (T_4 - T_1) - (T_3 - T_2)$$

clock offset:

$$\Theta = \frac{(T_2 - T_1) + (T_3 - T_4)}{2}$$

from GPS, are termed stratum 1. They distribute time to clients that can themselves be servers: a server receiving time from a set of stratum N receivers would be stratum $N+1$. Internet servers receive billions of requests per day from tens of millions of users, if not hundreds of millions. Along with simply setting the date on computers, network time protocol is widely used in all sorts of networks for such purposes as database management and official time-stamping. Specified by the Internet Engineering Task Force (IETF), computer code and information can be found in www.ntp.org, and the writings of David Mills [6]. Network time protocol is initiated when a client computer sends a small packet to a time server. Minimized through use of

universal datum protocol (UDP), the packet contains little more than the client's time when it was generated and the return IP address. Upon receipt of the packet, the server shortly thereafter sends a return packet that contains the original time stamp, along with the server's time when it received the packet, and the time it sent off the return packet. The client records the return packet's time of reception. That is sufficient to estimate the difference between the server and client clocks, and the roundtrip travel time, assuming that the travel-time over the Internet was the same in both directions (Figure 1).

The error budget is dominated by the network travel-time asymmetry, which would be expected to be larger for more-distant servers. Figure 2 shows that nearby servers are slightly more stable in a statistical sense [7]. However, many forms of deviations are not always captured by the statistics, and an example of a transient effect is shown in Figure 3 [7]. Here, the observed difference between a server in St. Louis, Missouri, and one at the US Naval Observatory became bimodal and biased at the level of tens of milliseconds. Three other Washington clients observed variations over the same period, which differed considerably in detail among themselves. Still larger variations, persistent over weeks, have been observed between continents; again, they appeared with different patterns and magnitudes for different clients, who coincidentally had different platforms and versions of the network time protocol installed. Editing data on the basis of excessive roundtrip travel time can identify bad time transfer exchanges. Not always, but in the case of Figure 3, deleting the sections with high round-trip delays would have been useful in removing the bimodal behavior, although a bias would have remained.
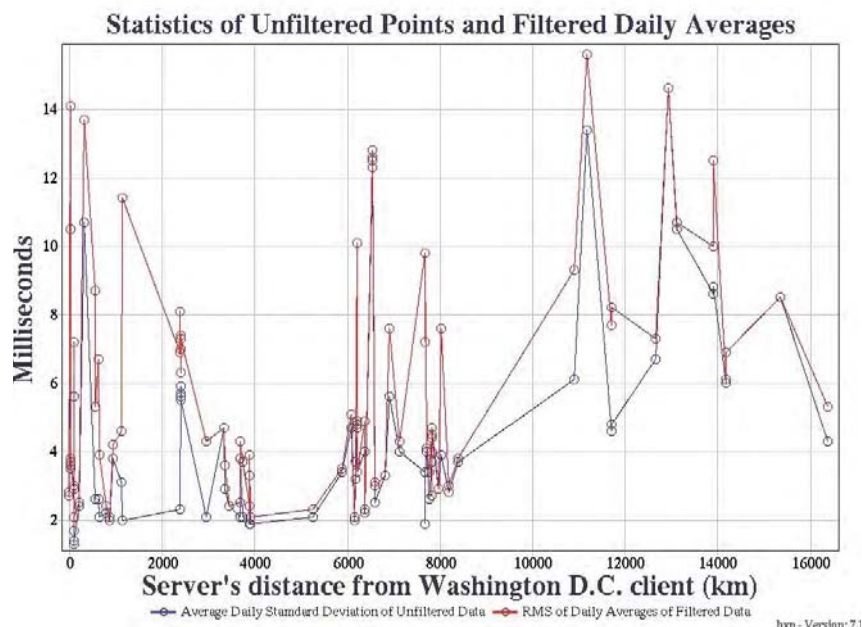

Figure 2. The filtered daily and unfiltered sub-daily standard deviation of network time protocol as seen by a Washington DC client. Pool servers were arbitrarily assigned a distance of 111 km (one degree in latitude).

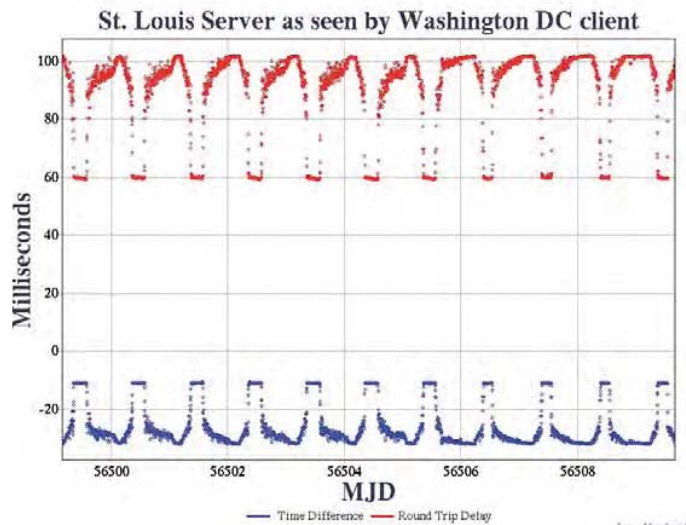**St. Louis Server as seen by Washington DC client**

Figure 3. A timing error pattern of a server in St. Louis, Missouri, as seen by a client referenced to UTC (USNO) in Washington, DC [7]. The red upper curve is the round-trip travel time over the Internet; the blue lower curve is the observed timing difference from UTC (USNO). MJD, the modified Julian date, is the number of calendar days since November 18, 1858.

In recent years, a demand has grown for authenticated network time protocol, by which the identity of the server is cryptographically verified. Several laboratories offer this service, occasionally via a for-profit third party. Unfortunately, authentication cannot protect against server failure. Authentication would also still not protect against situations in which an intermediate network component systematically delays packets traveling in one direction. Authentication could become vulnerable to exploitation of cryptographic collisions, enabling a would-be saboteur to rewrite signed time-stamps in an undetectable manner, although the distributed manner in which packets travel over the Internet would offer some protection. It is always recommended that clients always use several redundant servers for an integrity check. Some providers, such as NIST and others listed in www.pool.ntp.org, offer a service that pools servers so that a client randomly points to a variety of nearby servers.

The network time protocol format carries leap-second notifications, for which a table created at NIST has become an industry standard [8]. Unfortunately, every recent implementation of a leap second has resulted in many servers giving false time, sometimes for one day or longer. Conversely, it has been reported by an authoritative but unpublished source that since 2008, on every December 31 and June 30 when a leap second was not in fact called for, some server somewhere in the world erroneously set the leap second indicator [9].

Another widely used network time-transfer method is precise time protocol (PTP). In its full implementation, precise time protocol sends packets to set the time of each component in the network, whereas network time protocol simply passes through the components along the way. Since each component is set to the time of a topologically adjacent unit, network asymmetry is no longer a factor. Furthermore, the instrumental delays associated with each component's asymmetry are modeled, and the error in going from the

ports to the logical center of the component is avoided by measuring time at the physical interface. Precise time protocol is designed for controlled local networks, and time-transfer accuracies of tens of nanoseconds can be obtained [10, 11]. However, on the Internet, non-precise-time-protocol-compatible components degrade the accuracy to the same level as network time protocol [11]. To benefit from all the precise time protocol improvements on the decentralized Internet, implementation would also require a means to protect against "spoofers" spreading false time to nearby components.

3. GNSS Time Transfer

Global navigation satellite systems, or GNSS, provide an extremely reliable way of determining the synchronization errors of ground clocks with respect to each other. In the absence of interference, GNSS signals are continuously available, everywhere in the world. After correction for the atmospheric perturbations encountered by the signal, the GNSS measurements will give access to the timing difference between the laboratory ground clocks and the reference time scale conveyed by the atomic clocks onboard the GNSS satellites $(t_{local} - ref)$. Computing the differences between these quantities collected in two remote sites provides the synchronization between the two remote clocks, and the time evolution of the behavior of the clocks relative to each other. For users unable to afford redundancy or even a ground clock, expenses could be limited to an antenna and a receiver, as shown in Figure 4.

3.1 Time-Transfer Standard

Initially (starting in the eighties) GNSS time transfer was mainly realized using GPS C/A code observations collected by single-channel receivers, and using the satellite positions and clocks provided in the navigation messages
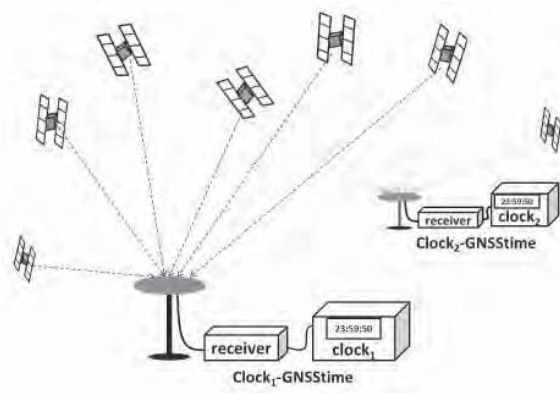
Figure 4. A schematic diagram for GNSS time transfer. The majority of links used in International Atomic Time generation are based upon this configuration. Data from the GNSS receiver, and data comparing the receiver's reference clock to all other laboratory clocks, are digitally uploaded to the BIPM (Bureau International des Poids et Mesures).

[12]. The solutions $(clock_i - ref)$ were collected in dedicated files using the CGGTTS format (for Common GPS GLONASS Time Transfer Standard [13, 14]). These solutions corresponded to a smoothed 13-minute solution for the satellites and epochs appearing in a dedicated tracking schedule provided by the Bureau International des Poids et Mesures (BIPM). Following the improvements of atomic frequency standards in terms of precision and accuracy, the removal of selective availability, and stabilization of the full constellation so that 8/9 satellites were usually available, GPS (or more generally, GNSS) time and frequency transfer underwent major evolutions, both at the algorithmic and hardware levels. Among these was the introduction of multi-channel receivers (e.g., [15]), which increased the number of satellites and correspondingly reduced the noise of clock solutions. Applications requiring the highest precision, such as the computation of International Atomic Time, benefited by correcting the broadcast satellite orbits, satellite clocks, and ionosphere model with the more-precise products computed by the International GNSS Service (IGS) [16, 17]. A variety of troposphere models could be used, and the BIPM uses the hydrostatic Saastamoinen model, which was described in the International Earth Rotation Service (IERS) conventions [18]. The method was later upgraded to benefit from the dual-frequency receivers that observe both GPS frequencies and extract the ionospheric delays to the first order (i.e., 99% of the effect) [19]. The ionosphere-free dual-frequency combination is named P3, and its use led to a factor of two improvement in the stability of the intercontinental time links up to averaging times of 10 days (e.g., [20]). Presently, this approach constitutes the state of the art in GNSS time transfer using only code measurements. The stochastic uncertainty (U_A) is at the level of a few nanoseconds, being limited by the current noise and multipath of the code measurements.

3.2 Common View and All-in-View

The initial Common GPS GLONASS Time Transfer Standard files were produced by single-channel GPS receivers. The time transfer was named "common view" (CV) as it was computed as the differences of the Common GPS GLONASS Time Transfer Standard results collected simultaneously from the same satellite by the two stations:

$$\Delta T = C1 - C2 \qquad (1)$$

$$= \frac{1}{N}\sum w_i \left[(G - C_1)_{i1} - (G - C_2)_{i2} \right],$$

where ΔT is the inferred time difference between the clocks C_1 and C_2, and $(G - C_n)_{in}$ is the observed time difference between the GPS time (G) and the reference clock at that site (C_n), as determined from GPS satellite i measurements at site n. This computation is done at each observation epoch, the summation is over the N satellites in common view at both sites, and the assigned weight, w_i, is often taken as unity.

All the satellite hardware delays and satellite clock errors are cancelled in this technique; the remaining errors are mainly due to the errors in the corrections applied to the code measurements. When multi-channel receivers began to be implemented in the timing laboratories, common view used a weighted average of those satellites visible at both stations in each 13-minute track of the BIPM schedule. Since the number of simultaneously observed satellites decreases as the baseline increases, the quality of the common view solutions tends to degrade with increasing distance between the stations. Since the exclusion pattern systematically includes certain portions of the sky, systematic errors, such as multipath, would have link-dependent effects not adequately compensated for in calibrations based upon small-baseline full-sky observations. To avoid these problems, the BIPM switched to a technique once termed "melting pot," but now termed "all-in-view" (AV). A clock solution $(clock - ref)$ is computed at each epoch, independently for each station, using all visible satellites, and the difference of the solutions of the two stations is then computed afterwards, as follows:

$$\Delta T = C1 - C2 \qquad (2)$$

$$= \frac{1}{N}\sum w_i (G - C_1)_{i1} - \frac{1}{M}\sum w_i (G - C_2)_{i2},$$

where N and M are the numbers of observed satellites at stations 1 and 2. Since the errors from the satellite clock
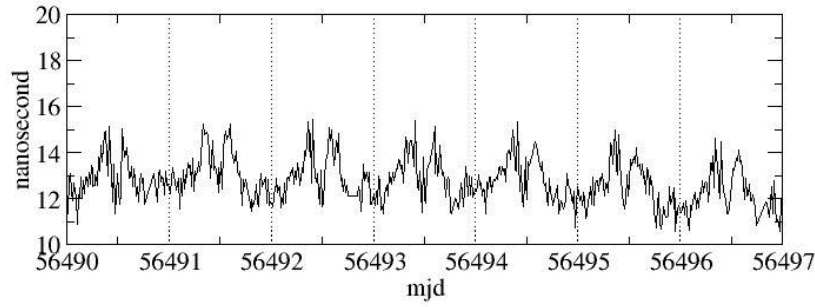
Figure 5. ROA-PTB (the link between the Spanish and German timing laboratories) computed with P3 and all-in-view by the BIPM (available on the BIPM ftp), showing the diurnal repeatability associated with the local environment (multipath plus possible temperature variations).

estimate and the ephemeris estimate do not cancel, as they do in the common-view technique, it is important to use precise ephemerides and clocks, rather than the broadcast navigation messages. Using IGS rapid products [17], the remaining uncertainties due to satellite orbits and clocks appropriately average to well below 100 ps for averaging periods of one day and longer [21, 22]. The references also document the significant superiority of all-in-view with respect to common view for baselines longer than 2000 km. As the baselines approach zero, all-in-view and common view become more equal. In modern GPS data reductions, the use of IGS products improves the data to a level wherein the uncertainties are dominated by multipath on the short term, and instrumental variations on the long term. For this reason, an elevation-dependent weighting is generally adopted in the all-in-view computations, giving more weight to observations at high elevations, i.e., less affected by multipath.

Since time transfer based on the Common GPS GLONASS Time Transfer Standard is a code-only analysis, both all-in-view and common view are significantly affected by multipath of the code signals [23]. Nanosecond-level diurnal variations can appear in the time-transfer solution. This is illustrated in Figure 5, for the link between Spain's timing laboratory ROA and Germany's counterpart (PTB) (about 2000 km). These variations were not due to the clocks. They were the signature of the code multipath (which would not be sinusoidal) and environmental sensitivity in one or both stations (which would usually be somewhat sinusoidal). The geometrical relationship among the satellite, the receiving antenna, and the reflectors that are the cause of multipath reflections has an approximate period of one sidereal day (about 23 h 56 min), so that the amplitude of the multipath signal for each satellite also has this periodicity. However, the pattern can also vary over longer periods, due to weather-induced changes in the reflectivity in the antenna's environment. Systematic geometric effects can often be identified by comparing data as a function of satellite azimuth and elevation, as in [24].

3.3 Carrier Phase

In parallel, some GNSS receivers provide phase measurements of the carrier signal. Thanks to the short wavelength of this signal, the measurement noise and multipath error is about 100 times lower than the noise of the code measurements. For this reason, the potential of GNSS carrier phases for time and frequency transfer was studied and demonstrated by different authors [e.g., 25-27]. With respect to the code measurement, the carrier phase measurement contains an additional unknown ambiguity, which is an integer number of cycles of the carrier. This is constant during a continuous visibility of the satellite, and must be determined from the data. Due to signal-to-noise limitations, the ambiguity is typically determined as a fractional number, but some software provides the option to force the ambiguity to be an integer [28]. Since the phase inherently carries no time information, ambiguity must always shift the phase, and the use of carrier phase data improves only the frequency comparison, not the overall time. The equations for the pseudorange (P) and carrier phases at each frequency i (L) are

$$L = R + c\left(-\tau_s + \tau_r + \tau_t\right) - c\tau_i + N_i\lambda_i + \lambda_i\omega_i + n_{\phi i} \quad (3)$$

$$P = R + c\left(-\tau_s + \tau_r + \tau_t\right) + c\tau_i + c\tau_{di} + n_{Pi} \quad (4)$$

where R is the geometric distance from the antenna to the satellite, τ_s is the satellite clock error, τ_r is the receiver clock error, τ_t is the tropospheric delay, τ_i is the ionosphere delay, N_i is the phase ambiguity, λ_i is the wavelength, ω_i is the windup correction associated with the varying orientation of the satellite with respect to the receiver during this pass, $n_{\phi i}$ is the phase noise, τ_{di} is the instrumental code delay, and n_{Pi} is the code noise.
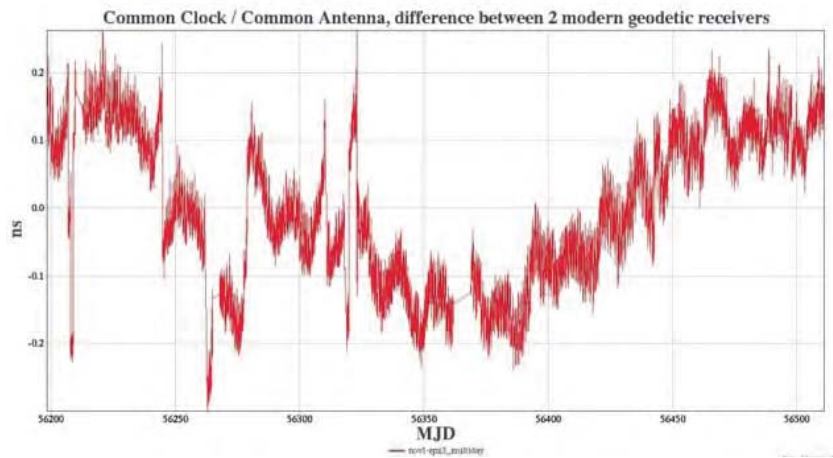
Figure 6. The observed calibration variations between two 21st-century geodetic GPS receivers. The variations may have been due to the electronics supplying the reference signals. Many older-model receivers have shown larger variations, and some somewhat shorter-duration comparisons of modern receivers have shown no discernable long-term variations and peak-to-peak noise < 20 ps.

The main analysis strategy used to combine code and carrier phase measurements for time transfer is the precise point positioning (PPP), as described in [29]. It requires correcting the data to a precision at least equal to that of the carrier phase measurements, using IGS satellite orbits and clock products, as well as Earth tide and ocean loading models [17]. The ionospheric delays are removed through the ionosphere-free combination of dual-frequency measurements, and the tropospheric delay of the dry atmosphere is modeled as in the Common GPS GLONASS Time Transfer Standard results. A fit is made to the data so as to determine and remove the receiver position, receiver clock, carrier phase ambiguities, and the delay due to the highly variable water vapor. While code-only data do not have the precision required to remove the wet delay, in precise point positioning one can either do this by fitting to the amplitude of an elevation-dependent mapping function and, as an option, to an azimuthal sinusoidal wet delay parameter, as well. Fortunately, precise-point-positioning-derived clock values have been shown to be very insensitive to the details of the mapping function employed, although the site clock, zenith troposphere delay, and antenna vertical position are highly correlated [30]. Due to the precision of carrier phase data and the ability to correct those data, precise point positioning can reach a U_A uncertainty of 200 ps for International Atomic Time generation [31], while five-minute points can have standard deviations as low as 15 ps.

The systematic uncertainty (U_B) for precise point positioning time transfer is equivalent to that from the Common GPS GLONASS Time Transfer Standard because the code data are the only observables providing access to the timing information of the clocks. On the one hand, the hardware delays are composed of the GNSS signal delay in the antenna, cable, and receiver, up to the receiver's internal timing measurement point. On the other hand, the time delay between the receiver's internal timing point and the external clock must be allowed for. The first part could be absolutely determined using a GNSS signal simulator, which creates a simulated signal of known time offset to pass through the receiving chain and to be measured. The U_B uncertainty on this kind of calibration is at the level of 1 ns on each frequency [32]. However, it requires specialized equipment that is rarely available. Instead, a relative calibration is usually used, in which a receiving chain is assumed to be absolutely calibrated, and then successively sent to the different laboratories to determine their hardware delays with respect to it. The uncertainty budget of the differential calibration technique is currently officially estimated to be 3.8 ns [33]. Although carefully done individual long-distance relative calibrations with precise point positioning have achieved total uncertainties of the order of 1 ns [34, 35], the BIPM's current policy is to use a conservative 5 ns as the U_B uncertainty for GNSS time transfer. This is under review [36], and any new standard must account for the inability to track system configuration changes at the several laboratories, as well as temporal variations of receiver calibration.

Common-clock observations of parallel GNSS receivers frequently revealed variations at the nanosecond or sub-nanosecond level over months, particularly in older models (Figure 6 and [37]). The use of redundant GNSS systems would enable laboratories to identify units with calibration jumps or drifts or that showed environmental sensitivity; receiver manufacturers have been known to improve their products based upon laboratory feedback (Powers, private communication).

The existence of seasonal calibration issues would be reflected in temperature- or humidity-related diurnal
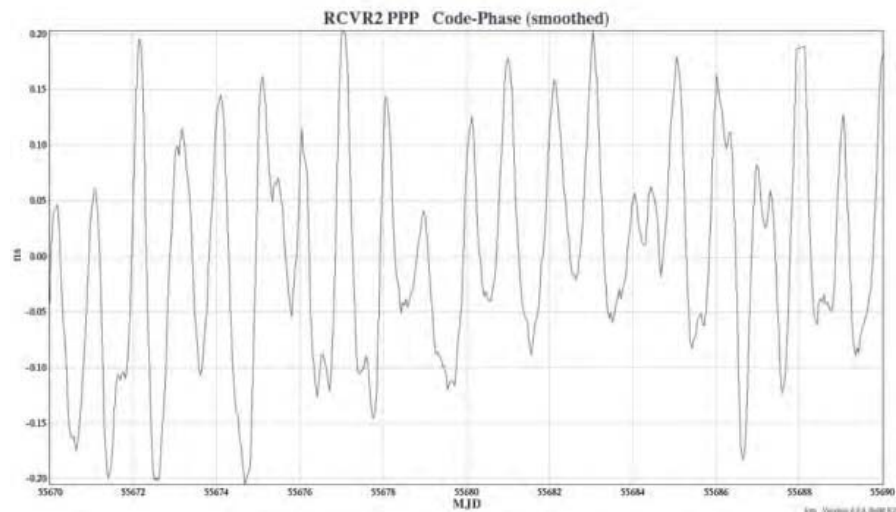
Figure 7. The signature of diurnal variations in the code as revealed in the solution residuals in precise point positioning processing. Such variations could be due to periodic interference, reflections, or expansion of the external cabling. Although often too weak to be seen in un-averaged data, they are suggestive of seasonal calibration variations. Note that the differencing was insensitive to all precise point positioning-derived parameters, except the ambiguities and ionospheric correction. Code residuals would retain sensitivity to all precise point positioning parameters, but any environmental effects that perturb code and phase equally would be absorbed into the clock parameters.

variations in GNSS receiver code data, as well as long-term changes of multipath. Sub-daily precise point positioning solutions are insensitive to daily code fluctuations. However, they can be seen in the solution code residuals (Figure 7 and [38]), along with other effects. These sub-daily code fluctuations are also the cause of the diurnal variations observed in the all-in-view solutions, and illustrated in Figure 5. The combined total of effects to which the code is most sensitive – including but not limited to multipath, interference, environmental dependencies – can lead to discontinuities at the boundaries of independent daily precise point positioning solutions. These are typically sub-nanosecond, and several techniques can reduce them [38-40]. However, the optimal situation is to design a station setup that reduces multipath, and especially the near-field multipath, which is the most problematic for time transfer [41]. One solution is to block reflected signals from entering the antenna. In Figure 8a, shield consisting of an RF absorber was placed below the antenna to prevent reflections from that direction. The impact of this reduced multipath could be seen by ranking all the stations of the IGS, where the station of Figure 8 (named BRUX) was among the three stations having the smallest rms of day boundary jumps [42].

When there are large inconsistencies between the carrier phase and the code, precise point positioning software can respond in predictable but often unexpected ways [43]. For example, Figure 9 shows the precise point positioning solutions for an extreme case, in which the receiver's phase data was apparently frequency offset from the code.

In addition to overall calibration variations, a variety of instrumental effects related to differences in the pre-correlation filtering of GNSS receivers can lead to systematic receiver and satellite-dependent biases at the sub-nanosecond and even nanosecond levels [44-46]. Averaging over different satellites will reduce the errors, but a detailed receiver-dependent analytic treatment is required for highly sub-nanosecond calibrations [47].

Figure 8. A GNSS antenna at the Royal Observatory of Belgium, designed with an underneath RF absorber to prevent near-field multipath.
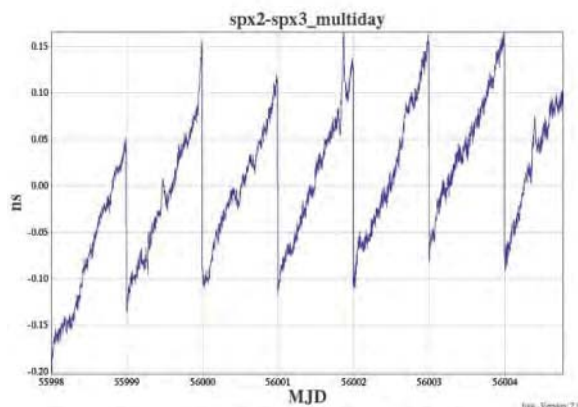
Figure 9. A precise point positioning solution difference between two receivers of the same make, with common clock and common antenna. The sawtooth variations became much smaller after a firmware upgrade, and were presumably due to a frequency offset in the phase data. The use of code data was able to correct this in the daily average, but not the sub-daily differences.
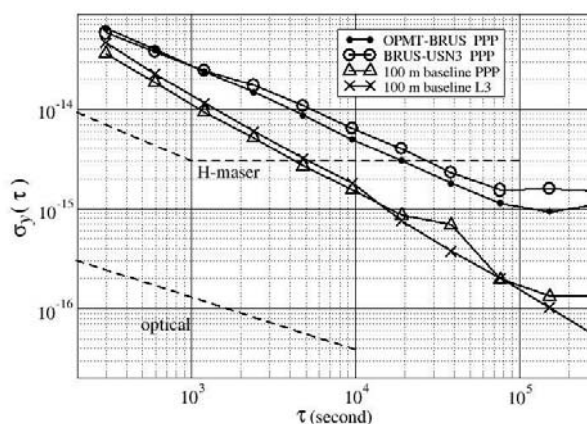

Figure 10. The Allan deviation of precise point positioning solutions compared to those of ground clocks. OMPT, BRUS, and USN3 are the IGS designations for geodetic GPS receivers maintained by the Observatory of Paris, the Royal Observatory of Belgium, and the USNO.

In order to illustrate the present possibilities of GNSS time and frequency transfer, Figure 10 presents the Allan deviations corresponding to some specific baselines. The two curves associated with the 100 m baselines were obtained using two separate receiving chains, both connected to the same H-maser. One curve resulted from the analysis of carrier phase data only (fixing the ambiguities to zero), while the second curve came from a precise point positioning analysis using the software developed by the National Research Council of Canada (NRCAN) on a multi-day basis, in order to avoid the day-to-day discontinuities inherent in daily processing of precise point positioning [39]. The difference between these two curves came from the use of code measurements that degraded the stability at intervals of a few hours, i.e., the classical duration of the satellite visibility on which the ambiguities were constant. Finally, the two last curves of Figure 10 present the Allan deviation of the precise point positioning solutions for the links Brussels-USNO (about 6000 km) and Brussels-Paris (about 300 km). Both provided approximately the same quality. However, the short-term stability was lower than what was expected from the 100-m baseline experiment; the origin of this degraded quality has not yet been identified to date. The H-maser stability curve in the figure shows that H-maser instabilities dominated over periods longer than three hours, so that the curves did not provide information about the performance of the technique. The optical clock stability curves showed that optical clock comparisons would be possible only for GNSS-data averaging times longer than several days, if at all.

3.4 Interoperable GNSS

A large improvement in GNSS capabilities is expected to ensue as new systems go online. By 2020, enough planned regional and global GNSS will have become fully operational so that almost 100 satellites will be globally accessible to users. The variety of signals will provide many opportunities for optimization, and an example of active work in this area was [48]. Figure 11 shows the current status in the Delhi sky for a constellation based upon 31 GPS, 24 GLONASS, four GALILEO, and 12 SBAS satellites augmenting GPS. Interoperability between systems will be particularly useful in cases where visibility is limited; in equatorial regions, ionospheric scintillation could also reduce the number of useful satellites [48]. To achieve full advantage of GNSS, the International Committee on GNSS (ICG) was formed in order to work out issues related to compatibility and interoperability, which are potentially confusing, since only GLONASS's internal reference time follows UTC (and therefore jumps with each leap second). In contrast, GPS and GALILEO times are continuous and 19 seconds offset from International Atomic Time (which has no leap seconds), while BEIDOU time is 33 seconds offset from International Atomic Time. In order to maximize the predictability of the GNSS system's time differences, the ICG requested a more real-time UTC reference, and this was a key motivation for the BIPM's creation of rapid UTC (UTCr).

The combination of measurements from different GNSS constellations for time transfer has several requirements. The receiver's internal reference must be the same for all systems, and the receiver system must be fully calibrated so that the hardware delays at its operating configuration are known for each signal transmitted by each constellation. In some cases, this is complicated by the fact the frequency bands used by different systems do not completely overlap, or the power spectrum inside the band is not the same. Finally, a key requirement concerns the reference of the satellite clock broadcast or corrected values. The user should either know the difference between the reference time scales at each observation epoch, or
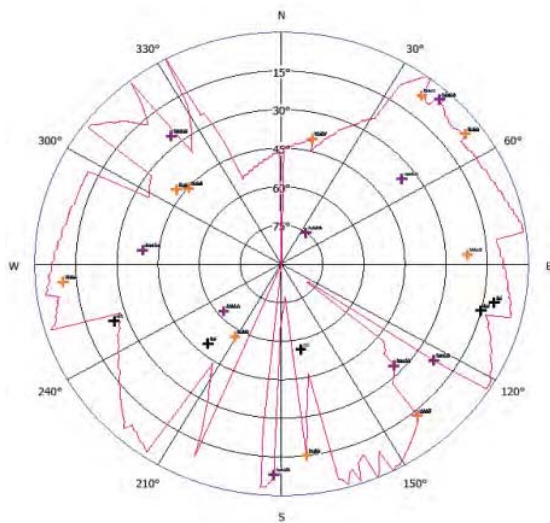
Figure 11. A typical instantaneous satellite pattern, with existing operational GNSS systems. The line segments represent the visibility limits set by nearby structures, the purple crosses refer to GPS Satellite 9, the orange crosses refer to GLONASS Satellite 10, and the black crosses refer to SBAS 5.

introduce this difference as an unknown to be estimated along with the other parameters.

Combined single-reference products are already provided for GPS and GLONASS satellites by some IGS analysis centers, and it is assumed that in the future, such products will also be provided for all GNSS. The combination of simultaneous observations of all these constellations in one global time transfer solution would therefore be possible. A user who fits to a constellation-wide bias could degrade the solution with unnecessary parameters, particularly for the epoch-averaged time-transfer difference. However, one possible benefit would be insensitivity to, and possible detection of, any un-modeled constellation-specific bias within the receiver.

The combination of GPS and GLONASS for time transfer has been studied for the all-in-view technique [49], and in precise point positioning [50]. Because GLONASS uses different carrier frequencies for each satellite, the hardware delays for each satellite-receiver pair must be determined in the clock solution. Since the advantage of increasing the number of observations is counterbalanced by the larger number of unknowns, combining GPS and GLONASS observations does not improve the time accuracy of the solution, although frequency variations are better determined. However, because each GPS, GALILEO, and BEIDOU satellite transmits on the same frequencies as the others in its constellation, their combination will increase the number of observations without increasing the number of unknowns per satellite. A theoretical improvement of a factor of $\sqrt{3}$ would in general be expected from the combination of GPS with the full GALILEO and BEIDOU constellations. The improvement would be still larger in cases of limited satellite availability, due to "dilution-of-precision effects."

Other improvements would be due to better atmospheric corrections, particularly because the frequencies used for the ionospheric correction are further apart for GALILEO. This has been confirmed by observations that the noise in reductions of GALILEO data using the ionosphere-free combinations of E1 with either E5a, E5b, or E5 AltBOC is significantly lower at all elevations than the noise of the ionosphere-free combination of the GPS P(Y)-codes on L1 and L2 [51].

4. LORAN

LORAN was developed for positioning during the second World War. LORAN is less precise than GNSS, due to variable and often un-measurable travel path and delay variations. The precision falls beyond 1000 km due to increased path and delay variations, decreased signal strength, and decreased angular spread of the transmitters. However, LORAN systems are much harder to jam, and could provide an important reliability factor for air and marine navigation. LORAN transmissions are given by chains of synchronized transmitting stations at low (100 KHz) frequencies, so that by observing a pair of stations, the observer can geolocate upon a hyperbolic track. By observing several pairs of tracks, the observer can determine a unique position. Although in its original design LORAN was not capable of delivering time or even time-of-day, in Enhanced LORAN, the hyperbolic solution is not used, since the signal is modified to transmit time information along with real-time corrections to LORAN
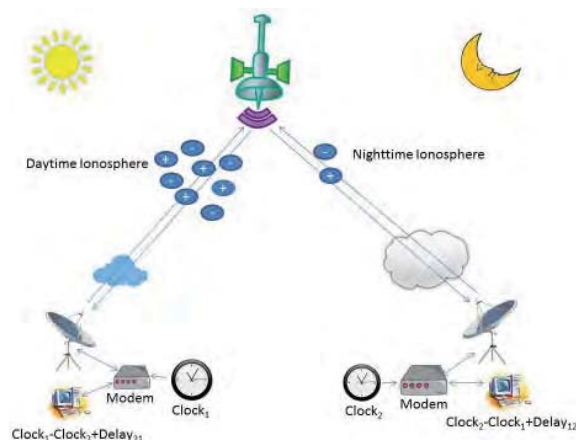

Figure 12. A typical TWSTT (two-way satellite time and frequency transfer) arrangement. Tropospheric cancellation is essentially complete, and the near equality of the uplink and downlink frequencies through each ionosphere leads to considerable cancellation. Satellite motion results in one direction having a slightly longer path length than the opposite direction. Time transfer is achieved by applying calibration and other corrections to the difference between the two modems' measurements of time-of-arrival minus time-of-transmission [53]. For International Atomic Time generation, the data from the modems are uploaded to the BIPM.

Figure 13. A portable two-way satellite time and frequency transfer (TWSTT) station, which is driven to remote sites for the purpose of calibration. The raised antenna ensemble on the taller roof is designed to minimize multipath. The large dish on the roof is capable of providing digital uplink information for GNSS systems, or conducting high-SNR two-way satellite time and frequency transfer observations.

data and the GPS broadcast ephemeris. The totality of these improvements will enable time delivery at the 10 ns level when differential corrections are used close to a transmitter [52]. This accuracy is sufficient for many marine and other applications, and therefore LORAN signals are routinely broadcast in Europe and Asia. Budgetary considerations led to the termination of the American program, although a limited amount of R&D work is still being undertaken in the United States, as well.

V. Two-Way Satellite Time and Frequency Transfer

Two-way satellite time and frequency transfer, or TWSTT, is currently rated by the BIPM as the best calibrated

of operational systems contributing to International Atomic Time. To conduct two-way satellite time and frequency transfer, a time-referenced spread-spectrum signal is transmitted to a geostationary satellite, where it is received and re-transmitted at a slightly different frequency to a cooperating user. That user simultaneously transmits a similar signal, which follows the inverse path to the first user (Figure 12).

The basic equations lead to a time difference between the reference clocks, T_i, for sites 1 and 2, as follows:

$$T_1 - T_2 = \frac{\left(\Delta T_1 - \Delta T_2\right)}{2} + \frac{\left(\tau_{1u} - \tau_{1d} - \tau_{2u} + \tau_{2d}\right)}{2}$$

$$+ \frac{\left(\tau_{1ut} - \tau_{1r} - \tau_{2t} + \tau_{2r}\right)}{2} + S, \qquad (5)$$

where for site i, ΔT_i is the counter reading, τ_{iu} and τ_{id} are the uplink and downlink signal delays including the path through the transponder, τ_{it} and τ_{ir} are the delay differences between the transmitting and receiving parts of the Earth station, and S is the Sagnac effect due to the non-reciprocity of the Earth's rotation.

Because the forward and reverse pathways are similar, many path delays are cancelled when the data at the two ends are differenced to form a timing difference. There remain sub-nanosecond errors in the path delay due to satellite motion, and due to the frequency difference between the upward and downward signals at each site, which lead to different sensitivities to the ionosphere, but these can be modeled [53]. If the satellite uses the same transponder to communicate with the two sites, then its
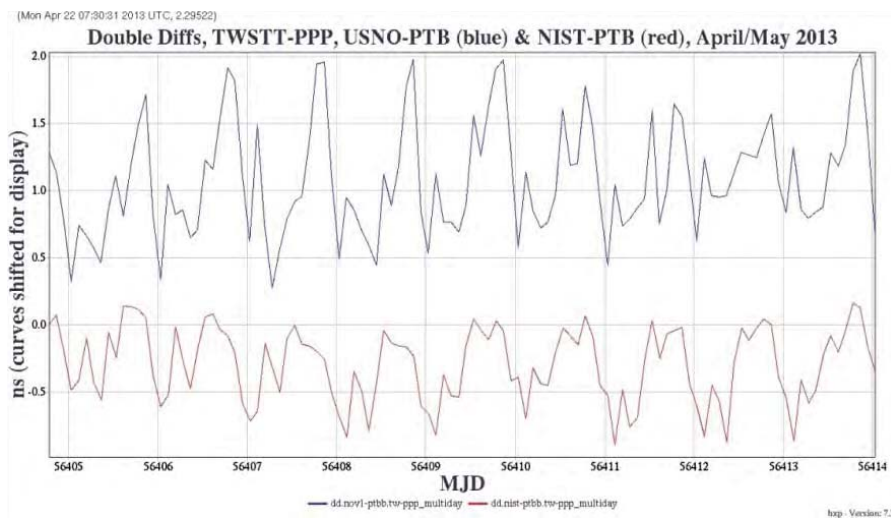

Figure 14. Diurnal signatures in two-way satellite time and frequency transfer between two North American labs and the PTB. To remove clock effects, the data were double-differenced with precise point positioning data. The pattern changed significantly in the following summer.
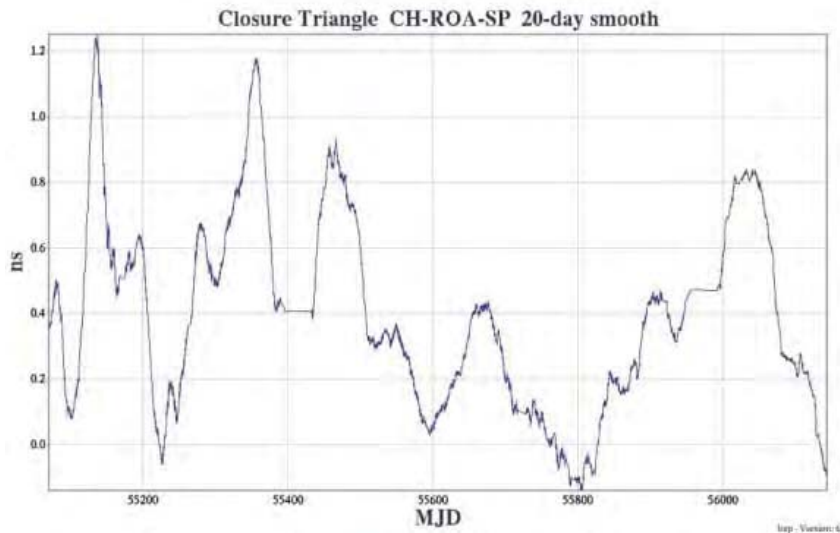
Figure 15. The closure sum of (CH-ROA), (ROA-SP), and (SP-CH). CH, ROA, and SP are the acronyms of the national timing labs of Switzerland, Spain, and Sweden, respectively. Independently of clock variations and all site-based calibration variations, the curve suggested a nanosecond-level limit to individual baseline stabilities.

contribution to the delays cancel, and the relative delay of the transmitting/receiving equipment can be measured by physically transporting a mobile system from one site to another, and conducting observations with the systems to be calibrated (Figure 13).

In most two-way satellite time and frequency transfer data, a lower limit to the short-term precision and the long-term accuracy is revealed by the presence of strong diurnal signatures, often at the nanosecond level (Figure 14). The strength and phase of these can vary with season, frequency, weather, baseline, equipment upgrades, and/or presence of other transmissions. No operationally useful causal relationship has yet been established, although Kalman filtering has been shown to be an effective filter for removing them [private communications from Koppang and from Jaldehag].

Some indications exist from closure studies that the monthly stability of two-way satellite time and frequency transfer calibrations is in general no better than one nanosecond [54]. To understand this, consider a complete set of all two-way satellite time and frequency transfer observations between three sites, whose semi-independent sets of measurements can be made, and their sum is given by

$$S = (A - B) + (B - C) + (C - A),$$ (6)

where A, B, and C are the times of reference clocks from laboratories A, B, and C; and S is the closure sum of the observations. The closure sum would be zero if all baselines were perfectly calibrated. If no site-based calibration was applied, the closure sum should be a constant, but it need not be zero because the observed delay is the average delay over the bandpass, which for each baseline is the product of the individual transmitting/receiving bandpasses [24, 55].

Equation (6) shows that any clock variations or source of error that is site-based (the same for the two baselines that a site is linked with) would not contribute to the closure sum, because the error would appear twice, with opposite sign. For triplets that use a common transponder, all atmospheric and environmental effects would cancel. Triplets that include more than one satellite transponder, such as transatlantic triplets, utilize different frequencies on different transponders, and this would lead to a small sensitivity to un-modeled ionospheric and site-based frequency-dependent variations. For all triplets, including those that employed different satellite transponders, the observed magnitude of the closure sum variations could be assumed to be less than the true calibration variations. Unfortunately, it is not possible from closure sums to know which baseline's calibration varied, but Figure 15 shows nanosecond variations of one European triplet of sites. Similar closure variations have been reported on Asian links, as well [W. H. Tseng, private communication].

Other ways to measure the stability of two-way satellite time and frequency transfer is through the constancy of repeat calibrations, and by double-differencing parallel observations. Two-way satellite time and frequency transfer calibrations are relative calibrations, in which the transportation and labor expenses cost several thousand Euros. Therefore, there have been very few repeat two-way satellite time and frequency transfer calibrations [56, 57]. These have generally been consistent with 1 ns repeatability, although a larger variation was reported in a recent paper [58].

Double-differencing parallel but otherwise independent two-way satellite time and frequency transfer observations provides a means to monitor stabilities. Again, due to the expense, such observation programs are rare. At least two cases of variations exceeding 3 ns over many months have been published [59]; however, as with GPS common clock

observations, the possibility of the delay variations being due to a component in the electronic infrastructure supplying the reference signals could not be ruled out.

Considerable effort has gone into the development of satellite simulators, which can enable the possibility of absolute calibration of two-way satellite time and frequency transfer systems. First developed at The Netherland's timing lab, VSL [60, 61], but also designed at the Observatory of Paris (OP) [63] and at at least one commercial entity, these would enable the measurement of the delay of each component, or set of components, of the system. They also would enable the identification of any component responsible for diurnal variations.

It is possible to combine two-way satellite time and frequency transfer with GPS, and the BIPM has created an operational product that uses precise point positioning data in the short-term but two-way satellite time and frequency transfer data for the long-term calibration [63]. While this merger would be vulnerable to any variations in the two-way satellite time and frequency transfer calibration, it retains the precision of precise point positioning, and is being used operationally in some circular-T links.

Two improvements to two-way satellite time and frequency transfer are being rapidly pursued, and show some promise. Observations employing carrier-phase have been shown to provide precisions of 1.E-16 at one day in common-clock short-baseline observations, and 2.E-15 at 1000 sec on the 10,000 km baseline between Japan's and Germany's timing labs (NICT and PTB) baseline (at which point the clock noise masks the performance; however, double-differences with precise point positioning data show relative agreement to 5.E-16 at one day) [64-66]. The noise of carrier phase two-way satellite time and frequency transfer is low enough that effects of satellite motion and differential ionosphere need to be fully removed, which requires the use of ranging data and either IGS products or their equivalents [67-68]. A second improvement to two-way

satellite time and frequency transfer under development is termed DPN, for dual pseudo-random noise [69]. This technique employs two narrow (~100 KHz) frequency bands that are widely separated (~ 20 MHz) for uplink and for downlink. The cross-correlation between their combinations yields timing information that is comparable to what would have been received if the full 20 MHz had been utilized. Time deviations (TDEVs) of 10 ps have been obtained at five minutes, and 70 ps at one day, while diurnals have disappeared.

6. Fiber-Optic Time and Frequency Transfer

Fiber-optic frequency transfer is an emergent technology under active development [5, 70]. Although it is usually not possible to calibrate fiber-optic systems over long distances without making justifiable assumptions about path symmetry, time transfer can be either verified or achieved through calibration with the other techniques.

The most common and best-developed method for long-distance fiber transfer can be termed two-way optical transfer (TWOT). Signals are transferred in both directions along a fiber-optic cable, and in one case comparisons with precise point positioning data has shown that the assumption of equal path lengths in each direction was sufficient to calibrate time transfer to the level of 100 ps, and this achieved frequency precision of 3.E-17 at one day [1] over a 480 km link. A demonstration of time transfer with absolute time accuracy of 250 ps and long-term timing stability of 20 ps was reported in [69], based on timestamps carried by the optical phase by modulating a very narrow optical carrier using two-way satellite time transfer modems. A similar technique was used on a 73 km baseline, reaching a time transfer accuracy better than 100 ps [72]. With a pulse-generator on an 80-km baseline, a Chinese effort demonstrated 50 ps time transfer at 1 second and 70 ps at 10,000 seconds [73].

Technique	Precision @5 min	Precision @1 day	Setup Cost	Operating Cost, Non-Labor	Major Improvements Underway
NTP	6 ms	4 ms	$2K	Minimal	PTP (local), pooling (Internet)
GNSS all-in-view (1 GNSS system)	3 ns	250 ps	$5-$20K	Minimal	Combined interoperable GNSS
GNSS PPP (1 GNSS system)	20 ps	100 ps	$10-$20K	Minimal	Multiple signals from multiple GNSS
LORAN	50 ns	100 ns	$5K	Minimal	Enhanced LORAN
TWSTFT (TWSTT)	150 ps	500 ps	$100K	~$100K/year	DPN, carrier-phase, simulators
Fiber-optic	1.E-17 s/s	1.E-19 s/s	$100-$200K	>>$100K/year	Operational use

Table 1. Crude estimates of the current best-practice post-processed operational performance of different techniques, taking advantage of readily available free resources such as IGS products. All quantities are variable by at least a factor of two. Although multiple systems are recommended, the setup costs are estimated for hardware at one system at one laboratory. The operating costs are only for satellite time and fiber-optic rental. Precision over a given time interval is defined in analogy with the Allan deviation, as the rms difference between adjacent data points averaged over that interval, divided by two.

A Japanese link between two optical frequency standards attained frequency precisions of 7.E-17 at 1000 s along a 45-km length at night [74]. European two-way observations over 146 km and 920 km links reached precisions of the order of 5.E-19 over hours and days [75, 76]. An intensive long-term two-way effort involving many European laboratories is in preparation.

SP (Technical Research Institute of Sweden) has developed a low-profile method for passive long-distance – and possibly even trans-oceanic – frequency transfer that was based upon timing the passage of the frame boundaries at the nodes. They reported a precision of a 1100 km in a sub-sea link as 1.E-15 at one day, or 100 ps [77]. One-way two-color transmissions, which compensated for fiber-delay variations by exploiting the frequency-dependent propagation speeds of the two colors, had precisions of 1.E-17 at one day over 6 km distances [78, 79], but the decorrelation of the noise limited the performance over long distances.

Although the expense of renting fiber-optic cables is usually quite high, the technical capabilities of this infant technology are rapidly expanding [80]. They have not reached their theoretical limits, such as in which the noise is proportional to the baseline to the 3/2 power of the distance, and inversely proportional to the frequency [81]. The startup costs for equipment could be as low as $50,000 for the simplest systems, such as the passive system developed by SP, or approach $500,000 for the highest-precision systems. Another potentially expensive cost is creating the connection between the laboratory port and the suitable commercial lines.

7. Conclusion

In this summary, we have made brief note of the advantages of each technique, which are often complementary. Table 1 attempts to describe the performance of the several techniques at their current levels of operational maturity. In order to deliver a reliable product for the user, timing laboratories must take into account all the elements discussed, along with customer capabilities and robustness, accuracy, and precision requirements. However the tradeoffs are made, time and frequency providers must foremost ensure the reliability of their own products. Redundant observations provide the most direct method of verification, as part of a package of both automated and manual quality-control checks. Care must be given at every step of the process, which for International Atomic Time generation is especially important at the systems at the pivot-laboratories that interconnect the time-transfer links of cooperating institutions [24].

8. Acknowledgements

9. Disclaimer

Neither the authors nor the institutions they support can endorse a commercial product. Any identifications would be for technical clarity only, and we caution the reader that the equipment properties described herein may no longer be characteristic of any equipment currently manufactured.

10. References

1. M. Lombardi, "Legal and Technical Requirements for Time and Frequency," *Measure*, **1**, 3, 2006, pp. 60-69.

2. L. Sliwczynski, P. Krehlik, A. Czubla, L. Buczek, and M. Lipnski, "Dissemination of Time and RF Frequency via a Stabilized Fiber Optic Link Over a Distance of 420 km," *Metrologia*, **50**, 2013, pp. 133-145.

3. S. Peil, S. Crane, J. Hanssen, T. B. Swanson, and C. R. Ekstrom, "An Ensemble of Atomic Fountains," Proceedings of International Frequency Control Symposium, 2012, pp. 1-4.

4. P. Gill, "Optical Frequency Standards," *Metrologia*, **42,** 2005, pp. S125-137; see also Gill's contribution to http://www.ptb.de/emrp/1393.html.

5. B. Warrington, "Next-Generation Frequency Standards," http://www.ieee-uffc.org/frequency-control/learning/pdf/Warrington-Next-generation_frequency_standards.pdf.

6. D. L. Mills., *Network Time Synchronization: The Network Time Protocol on Earth and in Space, Second Edition*, Boca Raton, CRC Press, 2011.

7. D. Matsakis, "NTP as Seen by the Users," Proceedings of ION-PTTI 2013, 2014.

8. Leap second information for NTP can be found below http://tf.nist.gov.

9. http://www.maths.tcd.ie/~dwmalone/time/leaps/.

10. R. Schmidt and B. Fonville, "A Network Time Protocol Stratum-1 Server Farm Fed by IEEE-1588," Proceedings of the 42nd Annual Precise Time and Time Interval (PTTI) Systems and Applications Meeting, November 16-18, 2010, Reston, Virginia, USA, 2011.

11. A. Novick, M. Weiss, K. Lee, and D. Sutton, "Examination of Time and Frequency Control Across Wide Area Networks Using IEEE-1588v2 Unicast Transmissions," 2011 Joint Mtg. IEEE Intl. Frequency Control Symposium and European Forum on Time and Frequency, 2011, pp. 670-675.

12. D. W. Allan and M. Weiss, "Accurate Time and Frequency Transfer During Common-View of a GPS Satellite," Proceedings IEEE Frequency Control Symposium, Philadelphia, PA, 1980, pp. 334-356.

13. D. W. Allan and C. Thomas, "Technical Directives for Standardization of GPS Time Receiver Software, *Metrologia*, **31**, 1991, pp. 69-79.

14. J. Azoubib and W. Lewandowski, "CGGTTS GPS/GLONASS Data Format Version," 27th CGGTTS meeting, 1998.

15. J. Levine, "Time Transfer Using Multi-Channel GPS Receivers, *IEEE Transactions on Ultrasonics, Ferroelectrics, and Frequency Control*, **46**, 2, 1999.

16. G. Petit and F. Arias, "Use of IGS products in TAI Applications," *Journal of Geodesy*, **83**, 2009, pp. 327-334.

17. Pointers to IGS data and products can be found at www.igs.org.

18. The IERS conventions can be found on www.iers.org; see also ftp://tai.bipm.org/iers/.

19. Z. G. Elmas, M. Aquin, H. A. Marques, and J. F. G. Monico," Higher Order Ionospheric Effects in GNSS Positioning in the European Region," *Annals of Geophysics*, **29**, 2011, pp. 1383-1399.

20. P. Defraigne and G. Petit, "Time Transfer to TAI Using Geodetic Receivers, *Metrologia*, **40**, 2003, pp. 184-188.

21. G. Petit and Z. Jiang, "GPS All-in-View Time Transfer for TAI Computation," *Metrologia*, **45**, 2008, pp. 35-45.

22. M. Weiss, G. Petit, and Z. Jiang, "A Comparison of GPS Common-view Time Transfer with All-in-View," Proceedings 2005 IEEE Frequency Control Symposium and Exposition (Vancouver, Canada), 2005, pp. 324-328.

23. P. Defraigne and C. Bruyninx, "Multipath Mitigation in GPS-based Time and Frequency Transfer, Proceedings European Forum on Time and Frequency, 2006, Braunschweig, Germany, 2006.

24. D. Matsakis, F. Arias, A. Bauch, J. Davis, T. Gotoh, M. Hosokawa, and D. Piester, "On the Optimization of Time Transfer Links for TAI," Proceedings of European Forum on Time and Frequency, Braunschweig, Germany, 2006.

25. T. Schildknecht, G. Beutler and M. Rotacher, "Towards Sub-Nanosecond GPS Time Transfer Using Geodetic Processing Techniques," Proceedings of the 4th European Frequency and Time Forum, 1998, pp. 335-346.

26. K. M. Larson, J. Levine, L. M. Nelson, and T. Parker, "Assessment of GPS Carrier-Phase Stability for Time-Transfer Applications," *IEEE Transactions Ultrasonics, Ferroelectronics, and Frequency Control*, **47**, 2, 2000, pp. 484-494.

27. C. Bruyninx and P. Defraigne, "Frequency Transfer Using GPS Codes and Phases: Short and Long Term Stability," Proceedings of the 31th Precise Time and Time Interval Meeting, 2000, pp. 471-478.

28. J. Delporte, F. Mercier, D. Laurichesse, and O. Galy, "GPS Carrier-Phase Time Transfer Using Single-Difference Integer Ambiguity Resolution," *International Journal of Navigation and Observation*, ID 273785, 2008.

29. J. Kouba and P. Héroux, "Precise Point Positioning Using IGS Orbit and Clock Products," *GPS Solutions*, **5**, 2, 2001, pp. 12-28.

30. U. Weinbach and S. Schon, "On the Correlation of Tropospheric Zenith Path Delay and Station Clock Estimates in Geodetic GNSS Frequency Transfer," Proceedings of the European Frequency and Time Forum, 2010.

31. G. Petit G, A. Harmegnies, F. Mercier, F. Perosanz, and S. Loyer, "The Time Stability of PPP Links for TAI," Proceedings Joint Meeting of the European Forum on Time and Frequency and IEEE International Frequency Control Symposium, 2011, pp. 1041-1045.

32. A. Proia, G. Cibiel, J. White, D. Wilson, and K. Senior, "Absolute Calibration of GNSS Time Transfer Systems: NRL and CNES techniques Comparison," Proceedings European Forum on Time and Frequency-International Frequency Control Symposium, San Francisco, 2011.

33. G. Petit, "Estimation of the Values and Uncertainties of the BIPM Z12-T Receiver and Antenna Delays for Use in Differential Calibration Exercises," BIPM Technical Memo 172, 2009.

34. H. Esteban, J. Palacio, F. J. Galindo, T. Feldmann, A. Bauch, and D. Piester, "Improved GPS-Based Time Link Calibration Involving ROA and PTB, *IEEE Transactions Ultrasonics, Ferroelectronics, and Frequency Control*, **57**, 3, 2010, pp. 714-20.

35. T. Feldmann, A. Bauch, D. Piester, M. Roster, E. Goldberg, S. Mitchell, and B. Fonville, "Advanced GPS Based Time Link Calibration with PTB's New GPS Calibration Setup," Proceedings of the 42nd Annual Precise Time and Time Interval (Precise Time and Time Interval) Systems and Applications Meeting, 2010.

36. Z. Jiang, G. Petit, and L. Tisserand, "Progress in the Link Calibration for UTC Time Transfer," Proceedings of the European Time and Frequency Forum, Prague, 2013.

37. Z. Jiang, D. Matsakis, S. Mitchell, L. Breakiron, A. Bauch, D. Piester, H. Maeno, and L. G. Bernier, "Long-Term Instability of GPS-Based Time Transfer and Proposals for Improvements," Proceedings of the 43rd Annual Precise Time and Time Interval (Precise Time and Time Interval) Systems and Applications Meeting, 2011.

38. D. Matsakis, K. Senior, and P. Cook, 2002, "Comparison of Continuously Filtered GPS Carrier Phase Time Transfer with Independent GPS Carrier-Phase Solutions and with Two-Way Satellite Time Transfer," Proceedings of the 33rd Annual Precise Time and Time Interval, 2002, pp. 63-87.

39. D. Orgiazzi, P. Tavella, and F. Lahaye, "Experimental Assessment of the Time Transfer Capability of Precise Point Positioning (PPP)," Proceedings International Frequency Control Symposium, 2005.

40. P. Defraigne, N. Guyennon, and C. Bruyninx, "GPS Time and Frequency Transfer: PPP and Phase-Only Analysis," *International Journal of Navigation and Observation*, 2009, Article 175468.

41. P. Defraigne, C. Bruyninx, "On the Link Between GPS Pseudo-Range Noise and Day-Boundary Discontinuities in Geodetic Time Transfer Solutions," *GPS Solutions*, **11**, 4, 2007, pp. 239-249.

42. https://timescales.nrl.navy.mil/IGStime/daybdy/.

43. D. Matsakis, M. Lee, R. Dach, U. Hugentobler, and Z. Jiang, "GPS Carrier Phase Analysis Noise on the USNO-PTB Baselines," Proceedings of the 2006 IEEE International Frequency Control Symposium, pp. 631-636.

44. C. Hegarty, E. Powers, and B. Fonville, "Accounting for the Timing Bias Between GPS, Modernized GPS, and GALILEO Signals," Proceedings of the 36th Annual Precise Time and Time Interval (Precise Time and Time Interval) Systems and Applications Meeting, 2005, pp. 307-317.

45. D. Matsakis, "The Timing Group Delay Correction (TGD) and GPS Timing Biases," Proceedings of the 63rd Annual ION National Technical Meeting, April 23-25, 2007, Cambridge, Massachusetts, USA (Institute of Navigation, Alexandria, Virginia).

46. D. Matsakis, S. Mitchell, and E. Powers, "Satellite Bias Corrections in Geodetic GPS Receivers," Proceedings of ION-PNT, Honolulu, HI, 2013.

47. B. Fonville, E. Powers, and D. Matsakis, "Determination of Early-Late Discriminator Errors on Filtered BPSK Waveforms," Proceedings of ION-GNSS, Nashville, TE, 2013.

48. P. Banerjee, A. Bose, and A. Das Gupta, "Effect of Scintillation on Timing Applications of GPS in Indian Subcontinent," *IEEE Transactions Instrumentations and Measurements*, **56**, 2007, pp. 1596-1600.

49. A. Harmegnies, P. Defraigne, G. Petit, "Combining GPS and GLONASS in All in View for Time Transfer," *Metrologia*, **50**, 2013, pp. 1-11.

50. P. Defraigne and Q. Baire, "Combining GPS and GLONASS for Time and Frequency Transfer," *Journal of Advances in Space Research*, DOI: 10.1016/j.asr.2010.07.003, 2011.

51. P. Defraigne, W. Aerts, G. Cerretto, G. Signorile, E. Cantoni, I. Sesia, P. Tavella, J. M. Sleewaegen, A. Cernigliaro, and A. Samperi, "Advances on the Use of GALILEO Signals in Time Metrology: Calibrated Time Transfer and Estimation of UTC and GGTO Using a Combined Commercial GPS-GALILEO Receiver," Proceedings of the Precise Time and Time Interval Systems and Applications, Bellevue, WA, December 3-5, 2013.

52. T. Celano, C. Biggs, B. Peterson, and K. Schmihluk, "Modernized LORAN-C Timing Test Bed Status and Results," Proceedings of the 36th Annual Precise Time and Time Interval (Precise Time and Time Interval) Systems and Applications Meeting, 2006, pp. 824-829.

53. D. Kirchner, "Two-Way Satellite Time and Frequency Transfer (TWSTFT): Principle, Implementation, and Current Performance," in W. R. Stone (ed.), *Review of Radio Science, 1996-1999*, Cambridge, Cambridge University Press, pp. 27-34.

54. D. Matsakis, L. Breakiron, A. Bauch, D. Piester, D., and Z. Jiang, 2009, "Two-Way Satellite Time and Frequency (TWSTFT) Transfer Calibration Constancy from Closure Sums," Proceedings of the 40th Annual Precise Time and Time Interval (Precise Time and Time Interval) Systems and Applications Meeting, 2009, pp. 587-604.

55. G. Hejc and W. Schaefer, "Tracking Biases Caused by Imperfections in DLL Receivers," Proceedings of the 42nd Annual Precise Time and Time Interval (Precise Time and Time Interval) Systems and Applications Meeting, 2011.

56. L. A. Breakiron, A. L. Smith, B. C. Fonville, E. Powers, and D. N. Matsakis, 2005, "The Accuracy of Two-Way Satellite Time Transfer Calibrations," Proceedings of the 36th Annual Precise Time and Time Interval (Precise Time and Time Interval) Systems and Applications Meeting, 2005, pp. 139-148.

57. D. Piester, A. Bauch, L. Breakiron, D. Matsakis, B. Blanzano, and O. Koudelka, "Time Transfer with Nanosecond Accuracy for the Realization of International Atomic Time," *Metrologia*, **45**, 2008, pp. 185-198.

58. T. Feldmann, A. Balu, S. Liu, W. Schafer, J. Achkar, and A. Kanj, "TWSTFT Calibration Involving Four Sites Using a Mobile Station on a Trailer," Proceedings of European Frequency and Time Forum, Prague, Czech Republic, 2013.

59. D. N. Matsakis, "Time and Frequency Activities at the US Naval Observatory," Proceedings of the 42nd Annual Precise Time and Time Interval (Precise Time and Time Interval) Systems and Applications Meeting, 2011, pp. 11-32.

60. G. DeJong, "Results in the Calibration of Earth Stations for TWSTFT Using the VSL Satellite Simulator Method," Proceedings of the 27th Annual Precise Time and Time Interval (Precise Time and Time Interval) Systems and Applications Meeting, 1996, pp. 359-372.

61. F. Mubarak and E. Dierikx, "Dual Stage Quad-Mixer Satellite Simulator for a TWSTSFT Station," Proceedings of Frequency Control and the European Frequency Time Forum (FCS), 2011, pp. 1-6.

62. J Achkar, "Design, Realization, and Application of a Satellite Simulator in a TWSTFT Station," 40th European Microwave Conference, 2010, pp. 1516-1519.

63. Z. Jiang and G. Petit, "Combination of TWSTFT and GNSS for Accurate UTC Time Transfer," *Metrologia*, **46**, 3, 2009, pp. 305-314.

64. F. Nakagawa, J. Amagai, R. Tabuchi, Y. Takahashi, M. Nakamura, S. Tsuchiya, and S. Hama, "Carrier-Phase TWSTFT Experiments Using the ETS-VIII Satellite," *Metrologia*, **50**, 2013, pp. 200-207.

65. M. Fujieda, T. Gotoh, M. Nakamura, R. Tabuchi, M. Aida, and J. Amagai, "Carrier-Phase-Based Two-Way Satellite Time and Frequency Transfer," *IEEE Transactions Ultrasonics, Ferroelectronics, and Frequency Control*, **50**, 12, 2012, pp. 2625-2630.

66. M. Fujieda, D. Piester, T. Gotoh, J. Becker, M. Aida, A. Bauch," Carrier Phase Two-Way Satellite Frequency Transfer over a Very Long Baseline," *Metrologia*, **51**, 2014.

67. B. Fonville, D. Matsakis, W. Shäfer, and A. Pawlitzki, 2005, "Development of Carrier-Phase-Based Two-Way Satellite Time and Frequency Transfer (TWSTFT)," Proceedings of the 36th Annual Precise Time and Time Interval, 2005, pp. 149-164.

68. S. Bryam and C. Hackman, "GNSS-Based Processing," ION-GNSS, 2011

69. W. H. Tseng, Y. J. Huang, T. Gotoh, T. Hobiger, M. Fujieda, M. Aida, T. Li, and S. Y. Lin, "First International Two-Way Satellite Time and Frequency Transfer Experiment Employing Dual Pseudo-Random Noise Codes," *IEEE Transactions Ultrasonics, Ferroelectronics, and Frequency Control*, **59**, 3, 2012, pp. 531-538.

70. G. Grosche, "Optical Frequency Transfer," http://www.ptb.de/emrp/1393.html.

71. O. Lopez, A. Kanj, P-E. Pottie, D. Rovera, J. Achkar, C. Chardonnet, A. Amy-Kleinand, and G. Santarelli, "Simultaneous Remote Transfer of Accurate Timing and Optical Frequency Over a Public Fiber Network," *Applied Physics B, Lasers and Optics*, 10.1007/s00340-012-5241-0.

72. M. Rost, D. Piester, W. Yang, T. Feldmann, T. Wübbena, and A. Bauch: "Time Transfer Through Optical Fibers Over a Distance of 73 km with an Uncertainty Below 100 ps," *Metrologia*, **49**, 6, 2012, pp. 772-778.

73. B. Wang, C. Gao, W. L. Chen, J. Miao, Y. Bai, T. C. Li, and L. J. Wang, "Fiber-Based Time and Frequency Dissemination Between THU and NIM," 2012 IEEE International Frequency Control Symposium, 2012, pp. 678-681.

74. M. Fujieda, M. Kumagai, S. Nagano, A. Yamaguchi, "An All-Optical Link for Comparison of Distant Clocks," *Optics Express*, **19**, 2011, pp. 16498-16507.

75. O. Lopez, A. Haboucha, B. Chanteau, C. Chardonnet, A. Amy-Klein, and G. Santarelli, "Ultra-Stable Long Distance Optical Frequency Distribution Using the Internet Fiber Network," *Optics Express*, **20**, 21, 2012, pp. 23518-23526.

76. G. Grosche, O. Terra, K. Predehl, R. Holzwarth, B. Lipphardt, F. Vogt, U. Serr, and H. Schnatz, "Optical Frequency Transfer via 146 km Fiber Link with 1.E-19 Relative Accuracy," *Optics Letters*, **34**, 2009, pp. 2270-2272.

77. S. C. Ebenhag, P. O. Hedenkvist, and K. Jaldehag, "Active Detection of Propagation Delay Variations in Single Way Time Transfer Utilizing Dual Wavelengths in an Optical Fiber Network," Proceedings of the 43rd Annual Precise Time and Time Interval (Precise Time and Time Interval) Systems and Applications Meeting, 2012.

78. J. Hanssen, S. Crane, and C. Ekstrom, "One Way Temperature Compensated Fiber Link," Proceedings of the Joint Conference of the IEEE Frequency Control Symposium and the 25th European Frequency and Time Forum, 2011, pp. 1-5.

79. S. C. Evenhag, P. O. Hedekvist, and K. Jaldehag, "Two Color One-Way Frequency Transfer in an Urban Optical Network," Proceedings European Frequency and Time Forum, 2013.

80. G. Grosche, S. M. F. Raupach, O. Terra, U. Sterr, H. Schnatz, A. Pape, J. Friebe, M. Ridemann, E. M. Rasel, S. Droste, K. Predehl, T. Udem, and R. Holzwarth, "Optical Frequency Transfer via Telecommunication Fibres," Workshop on Optical Networks for Accurate Time and Frequency Transfer, Hoofddorp, The Netherlands, November 20-21, 2012, http://www.ptb.de/emrp/1393.html.

81. P. A. Williams, W. C. Swann, and N. R. Newbury, "High-Stability Transfer of an Optical Frequency Over Long Fiber-Optic Links," *Journal of the Optical Society of America B*, **25**, 8, 2009, pp. 1284-1293